Electronic Supplementary Information

Amide-imine conjugate involving gallic acid and naphthalene for nano-molar detection, enrichment and cancer cell imaging of La^{3+}: Studies on catalytic activity of La^{3+} complex

Ahad Shaikh,[a] Milan Ghosh,[a] Pallabi Mukherjee[a], Avijit Ghosh,[b] Rostam Ali Molla,[c] Sabyasachi Ta*[a] and Debasis Das*[a]

[a]Department of Chemistry, The University of Burdwan, Burdwan, 713104, W.B., India

[b]Centre for Research in Nanoscience & Nanotechnology, (CRNN), University of Calcutta, Technology Campus, Sector-III, Block-JD 2, Salt Lake, Kolkata, 700098, West Bengal, India.

[c]Department of Science and Humanities, S. N. Bose Govt. Polytechnic College, Ratua, Malda, 73213, India

Materials and equipment

Chemicals and solvents are purchased from Sigma Aldrich. Always spectroscopic grade solvents and analytical reagent grade chemicals have been used without further purification. A Shimadzu Multi Spec 2450 spectrophotometer is used for recording UV-Vis spectra. FTIR spectra are recorded on a Shimadzu FTIR (model IR Prestige 21 CE) spectrophotometer. ^{1}HNMR and ^{13}CNMR spectra are recorded on a Bruker Advance 400 (400 MHz) spectrometer in methanol-d_4 and $CDCl_3$ respectively. Chemical shifts are reported in parts per million (ppm) and tetramethylsilane (TMS, δ 0.00) is used as reference. Multiplicity is indicated as follows: s (singlet), d (doublet), t (triplet), q (quartet), m (multiplet). Coupling constants are reported in Hertz (Hz). High resolution mass spectra are recorded on a Xevo G2S/Q-TOF. microTM spectrometer. Elemental analyses are performed on a Perkin Elmer 2400 CHN analyzer. The steady state emission and excitation spectra are recorded with a Hitachi F-4500 spectrofluorimeter.

General method of UV-Vis and fluorescence titration

A cells of 1.0 cm Path length used for absorption and emission studies. To measure UV-Vis and fluorescence titrations data, stock solution of **GAN** are prepared (20 μM) in DMSO/H_2O (4/1, v/v) HEPES (10 mM) buffer. Solutions of **GAN** and Lanthanum nitrate are altogether from respective stock solutions in definite concentration. 5 nm x 5 nm slit width is used to perform fluorescence measurements.

Job's plot from fluorescence data

A series of solution containing **GAN** and $La(NO_3)_3.6H_2O$ are prepared in such a way that the total concentration of La^{3+} and **GAN** remain constant (20 μM) in all the sets. The mole fraction (X) of **GAN** is varied from 0.1 to 0.9. The emission intensity at 472 nm is plotted against mole fraction of **GAN** in solution.

Estimation of detection limit

The detection limit (DL) is determined using the equation: $DL = \frac{3\sigma}{S}$ where σ is the standard deviation of the blank solution, S is the slope of the calibration curve.

Determination of quantum yield

Fluorescence quantum yields (Φ) are estimated by integrating the area under the fluorescence curves using the equation,

$$\phi_{sample} = \phi_{ref} \times \frac{OD_{ref} \times A_{sample} \times \eta^2_{sample}}{OD_{sample} \times A_{ref} \times \eta^2_{ref}}$$

where A is the area under the fluorescence spectra and OD is optical density of the compound at the excitation wavelength, η is the refractive index of the solvent used. In case of **GAN** the fluorescence quantum yield has been calculated in absence and presence of La^{3+} ion. The fluorescence quantum yield increases more than 21 times (λ_{em} = 472 nm) upon addition of 3.0 equivalent of La^{3+} ion to **GAN**.

Determination of binding constant

The binding constants of compound **GAN** for different analyte are determined using the following Benesi-Hildebrand equation.

$$\frac{F_{max} - F_{min}}{F_X - F_{min}} = 1 + \frac{1}{K[C]^n}$$

Where $\mathbf{F_{min}}$, $\mathbf{F_x}$, and $\mathbf{F_{max}}$ are the emission intensities of the compound **GAN** in absence of analyte, at an intermediate analyte concentration, and at a concentration of complete interaction with analyte respectively. **K** is the binding constant, **C** is the concentration of analyte and **n** is the number of analyte bound per probe molecule (here, **n** = 1). The value of **K** are obtained from the slopes of different plot for different analyte.

Cytotoxicity (MTT) assay

In vitro cytotoxicity is measured by using the colorimetric methyl thiazolyltetrazolium (MTT) assay against HeLa cells. Cells are seeded into 24-well tissue culture plate in presence of 500 μL Dulbecco's modified eagle medium (DMEM) supplemented with 10% fetal bovine serum (FBS) and 1% penicillin/streptomycin at 37ºC temperature and 5% CO_2 atmosphere for overnight and then incubated for 12h in presence of **GAN** at different concentrations (10-100 μM). Then cells are washed with PBS buffer and 500 μL supplemented DMEM medium is added. Subsequently, 50 μL 3-(4,5-dimethylthiazol-2-yl)-2,5-diphenyltetrazolium bromide MTT (5 mg/mL) is added to each well and incubated for 4h. Next, violet formazan is dissolved in 500 μL of sodium dodecyl sulfate solution in water/DMF mixture. The absorbance of solution is measured at 570 nm using microplate reader.

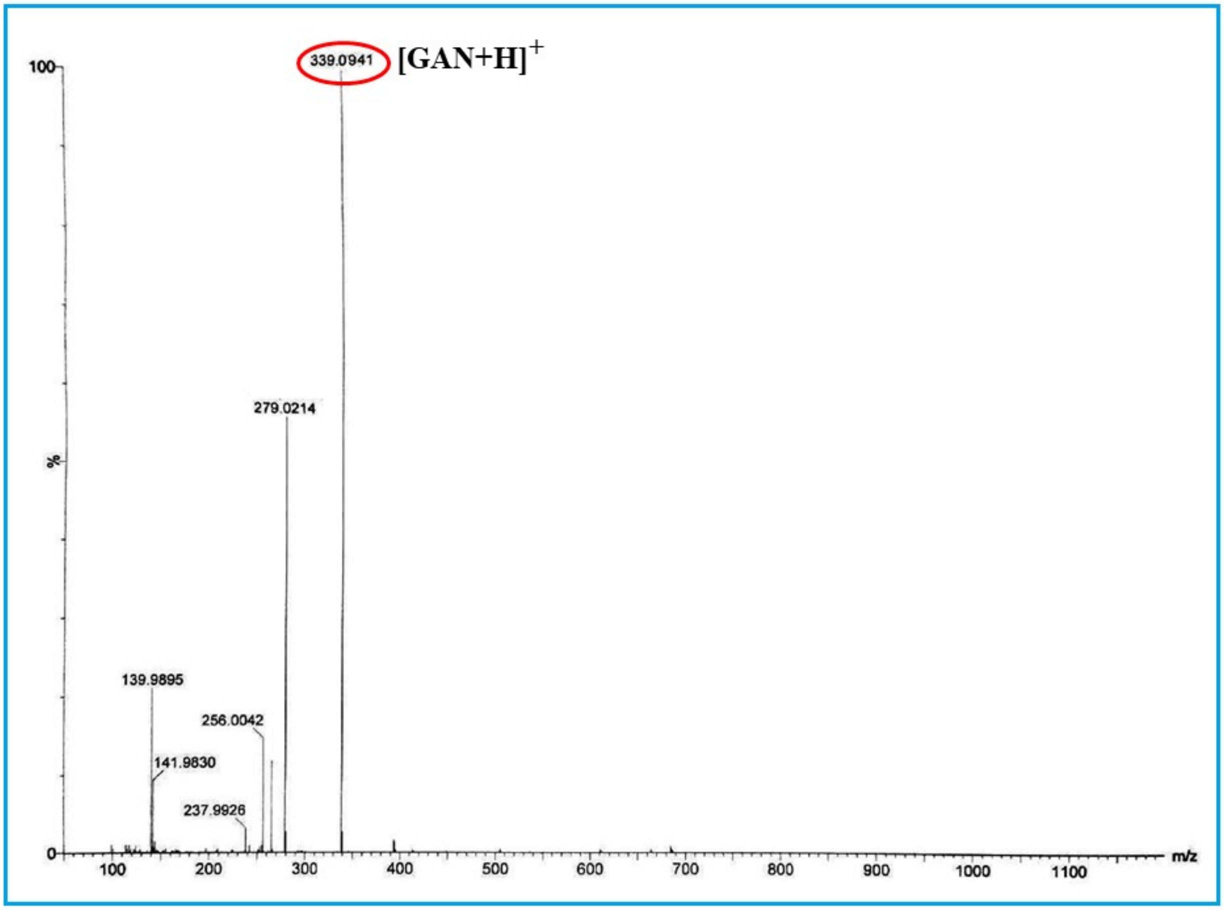

Fig. S1 ESI-MS of **GAN** in MeOH

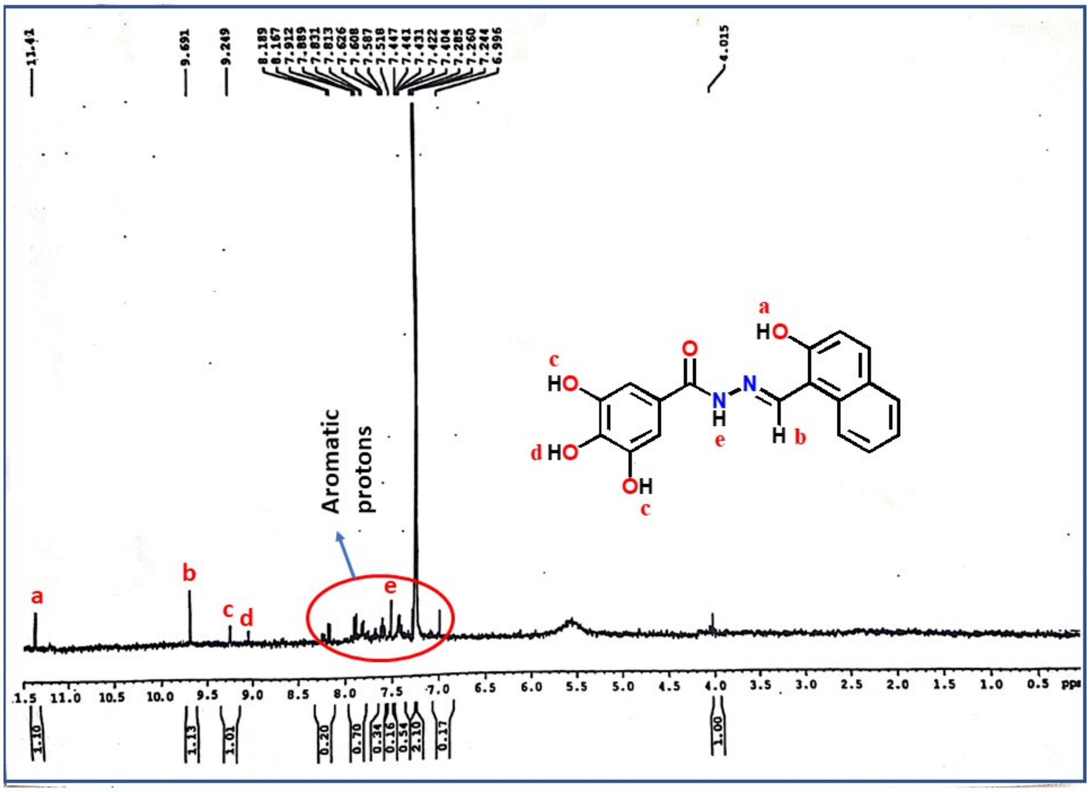

Fig. S2 ^{1}H NMR spectrum of **GAN** in $CDCl_3$

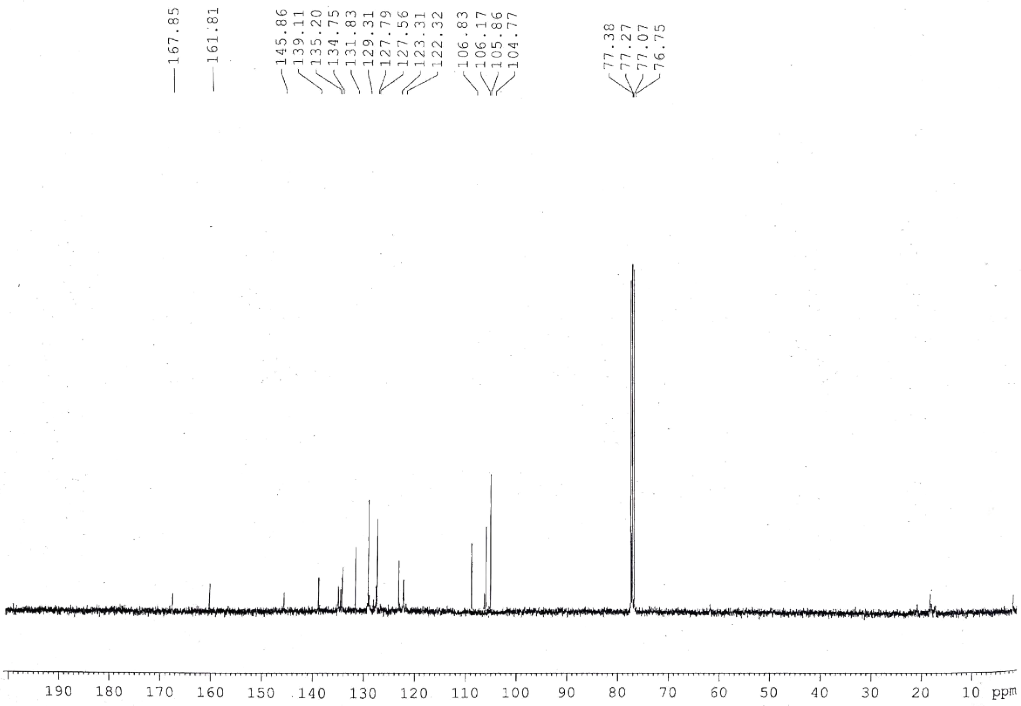

Fig. S3 ^{13}C NMR spectrum of **GAN** in $CDCl_3$

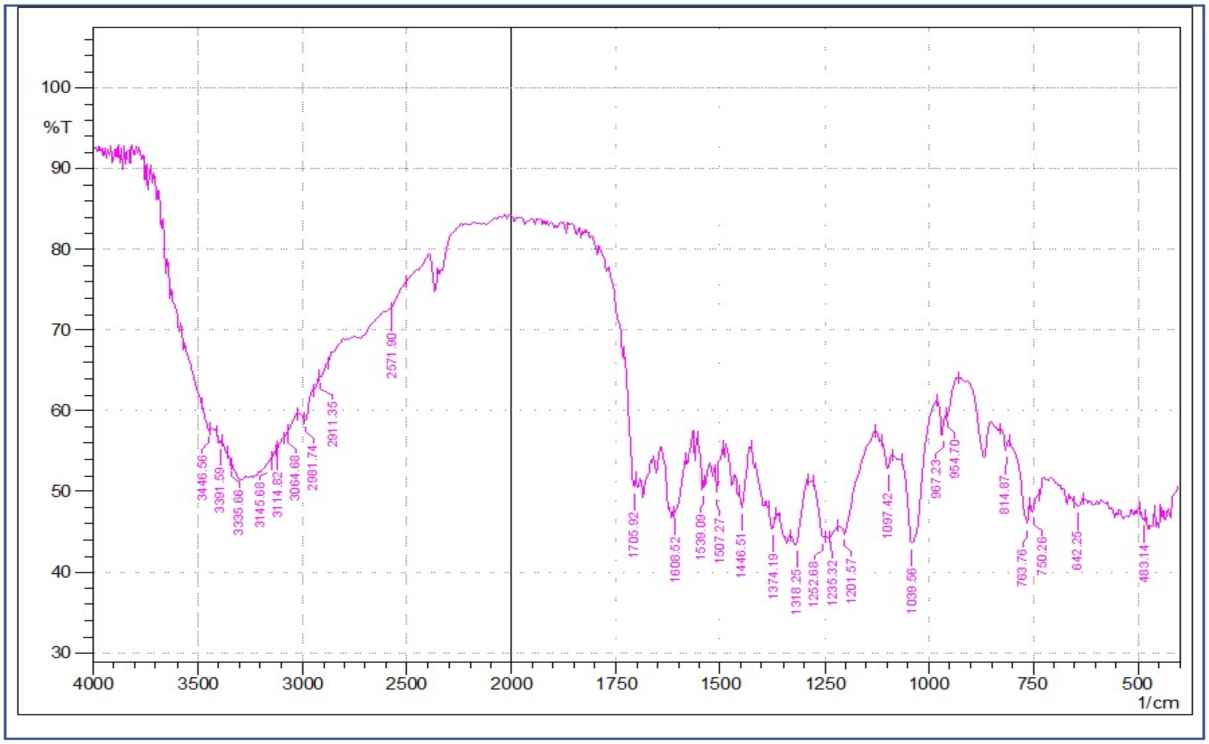

Fig. S4 FTIR spectrum of **GAN**

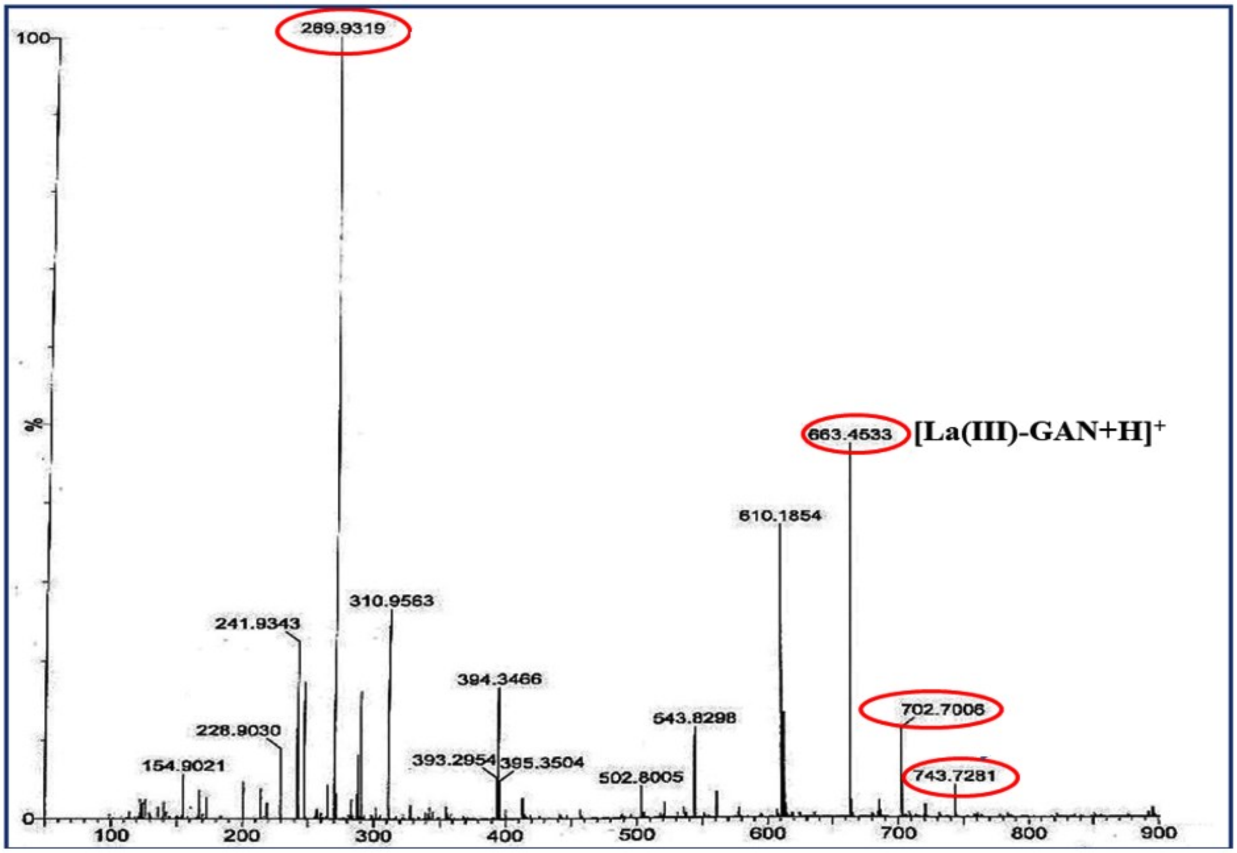

Fig. S5 ESI mass spectrum of [**La(III)-GAN]** complex

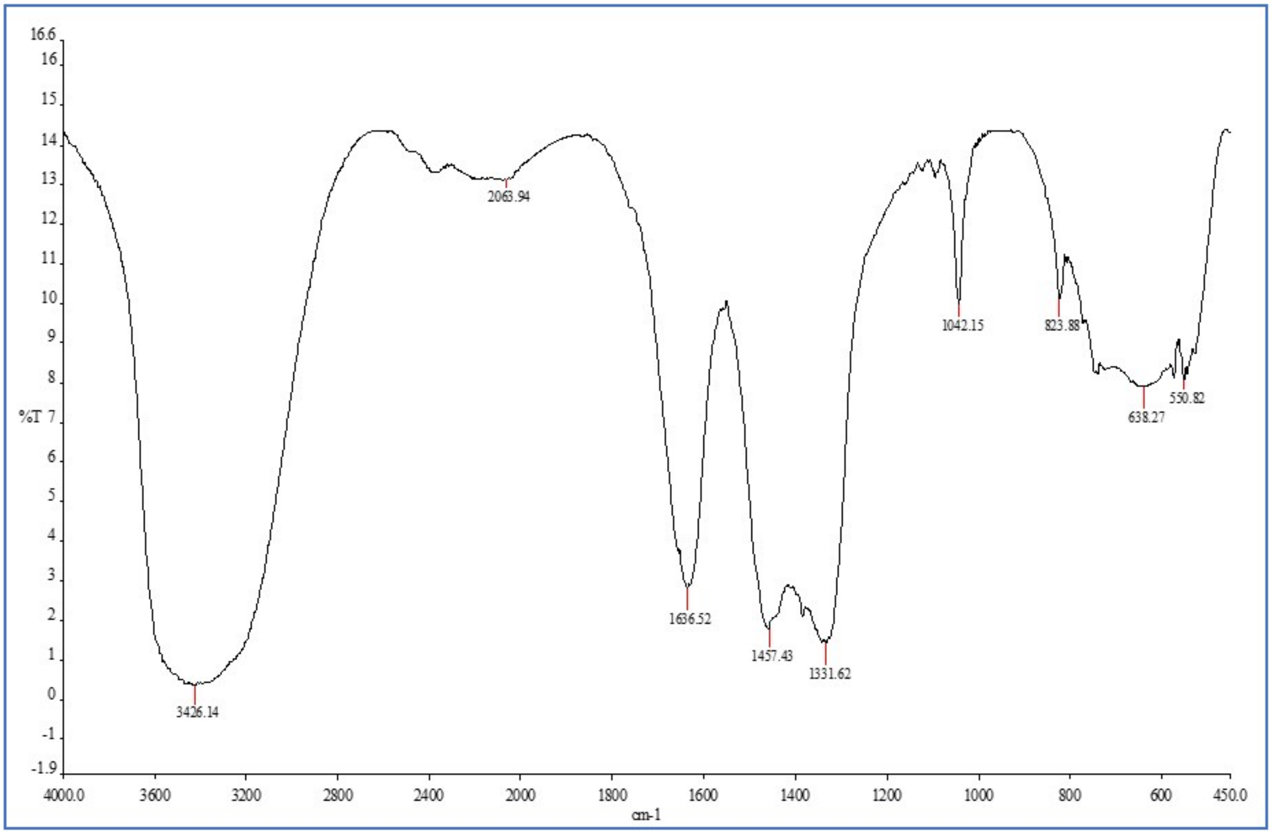

Fig. S6 FTIR spectrum of [**La(III)-GAN]** complex

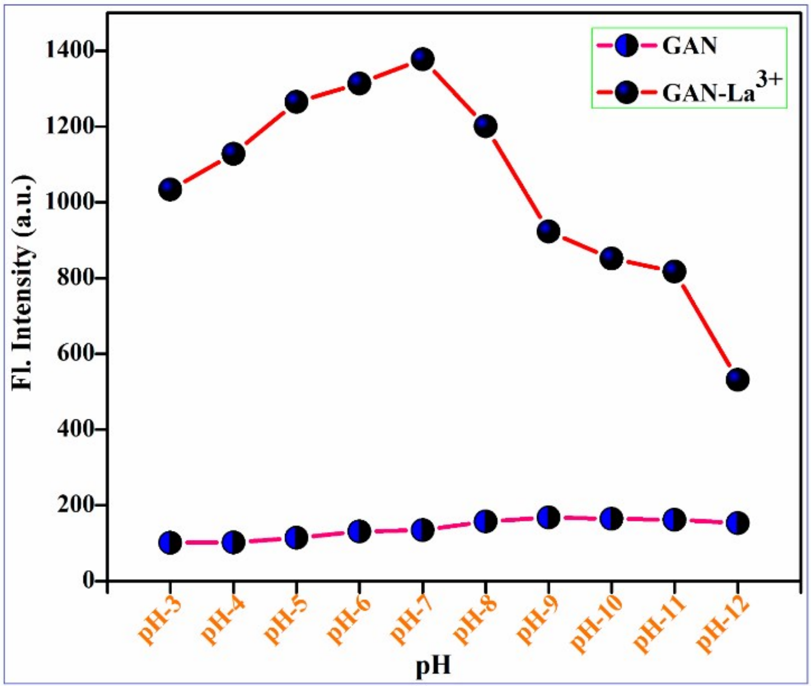

Fig. S7 Influence of pH on the emission profile of **GAN** (20 μM, DMSO/ H_2O, 4/1, v/v, λ_{em}, 472 nm) in presence and absence of La^{3+} ion

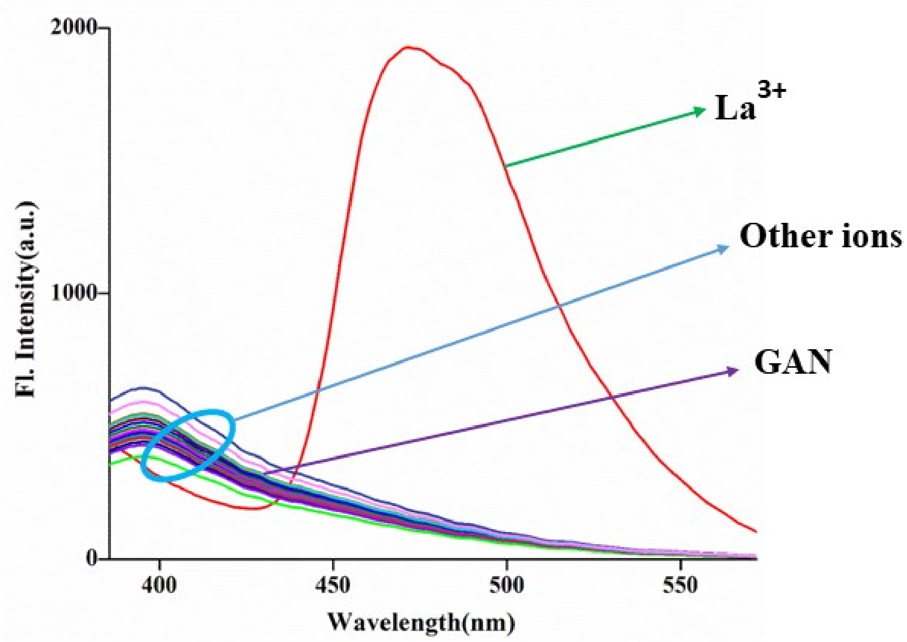

Fig. S8 Selectivity of **GAN** for La^{3+} and other cations

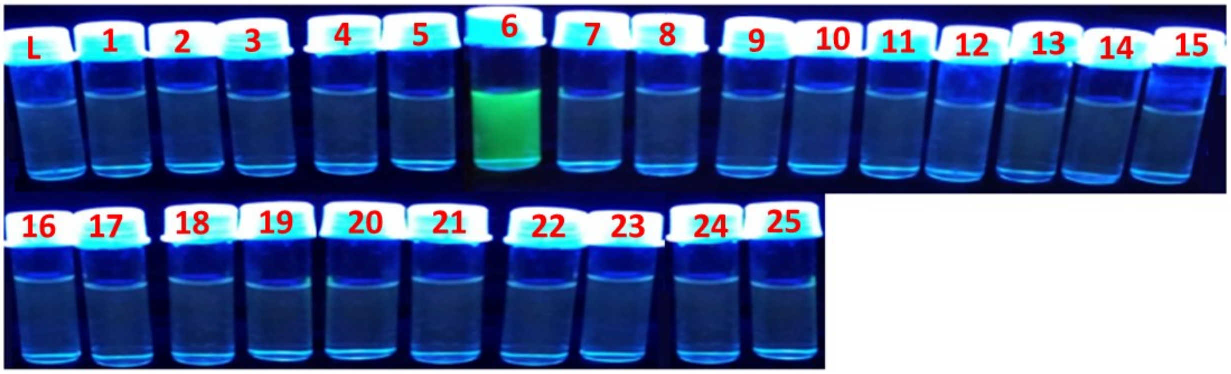

Fig. S9 Color of **GAN** (20 µM) in UV box in presence of different cations: 1- V^{3+}, 2- Cr^{3+}, 3- Mn^{2+}, 4-Co^{2+}, 5- Ni^{2+}, 6- La^{3+}, 7- Ce^{4+}, 8- Pr^{3+}, 9- Nd^{3+}, 10- Sm^{3+}, 11- Eu^{3+} 12- Gd^{3+}, 13- Tb^{3+},14- Dy^{3+}, 15- Ho^{3+}, 16- Er^{3+}, 17- Yb^{3+}, 18- Lu^{3+}, 19-Fe^{3+}, 20- Fe^{2+}, 21- Hg^{2+}, 22- Pb^{2+}, 23- Cd^{2+}, 24- Zn^{2+}, 25- Cu^{2+} (100 µM, DMSO/ H_2O, 4/1, v/v)

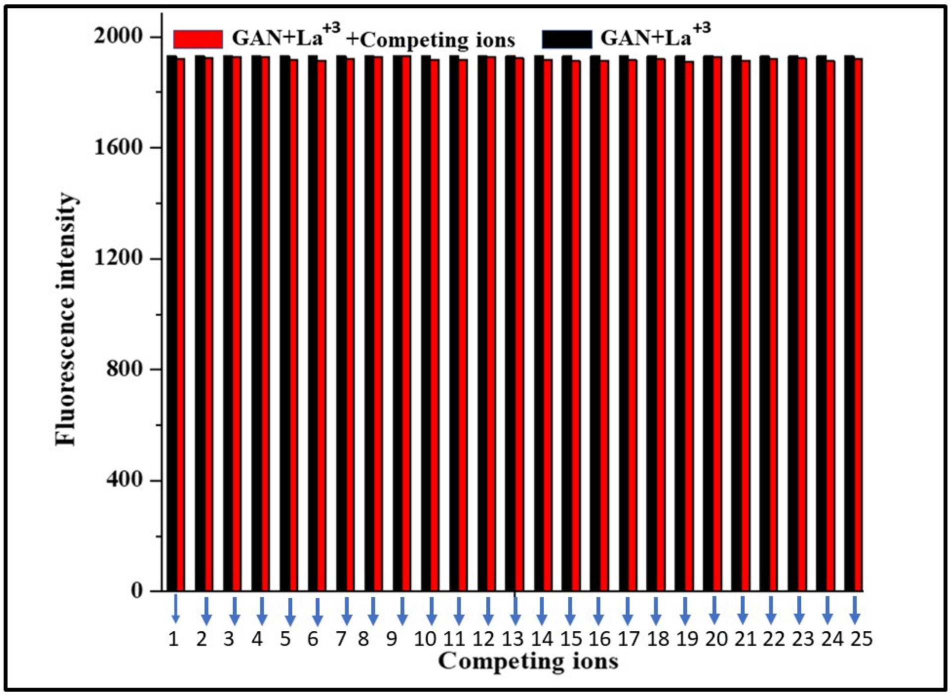

Fig. S10 Emission intensity of **GAN** (20 µM) in presence of different cations: 1- VO^{2+}, 2- Cr^{3+}, 3- Mn^{2+}, 4- Co^{2+}, 5- Ni^{2+}, 6- Cu^{2+}, 7- Fe^{2+}, 8- Fe^{3+}, 9- Hg^{2+}, 10- Pb^{2+}, 11- Al^{3+}, 12- Ag^{+}, 13- Zn^{2+}, 14- Cd^{2+}, 15- Ce^{3+}, 16- Pr^{3+}, 17- Nd^{3+}, 18- Sm^{3+}, 19- Eu^{3+}, 20- Gd^{3+}, 21- Er^{3+}, 22- Tb^{3+}, 23- Ho^{3+}, 24- Lu^{3+} and 25- Yb^{3+} (10 equiv., DMSO/ H_2O, 4/1, v/v, λ_{ex}, 336 nm)

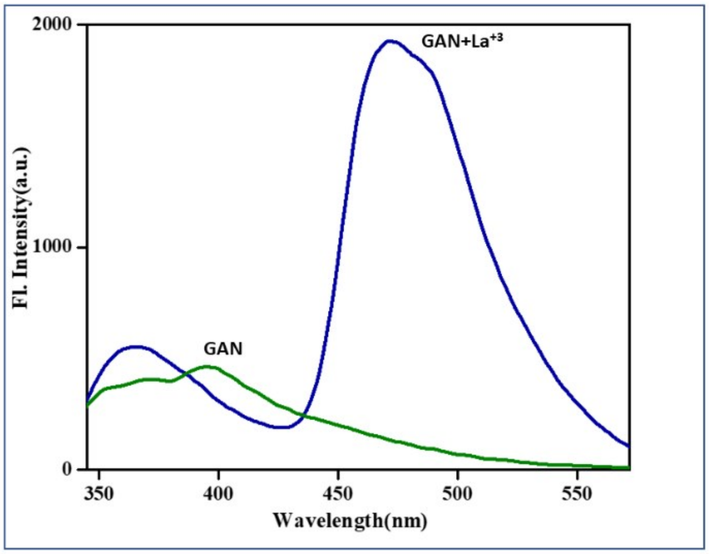

Fig. S11 Emission spectra of **GAN** and [**GAN**-La^{3+}] complex

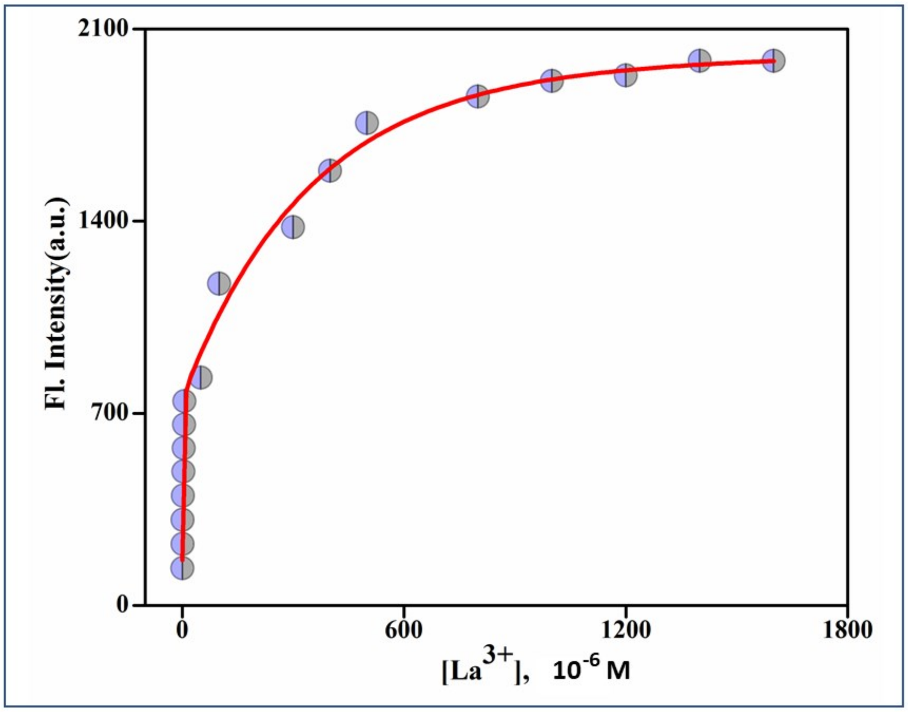

Fig. S12 Plot of emission intensities of **GAN** (20 μM) as a function of added La^{3+} ion (0-3000 μM) at 472 nm

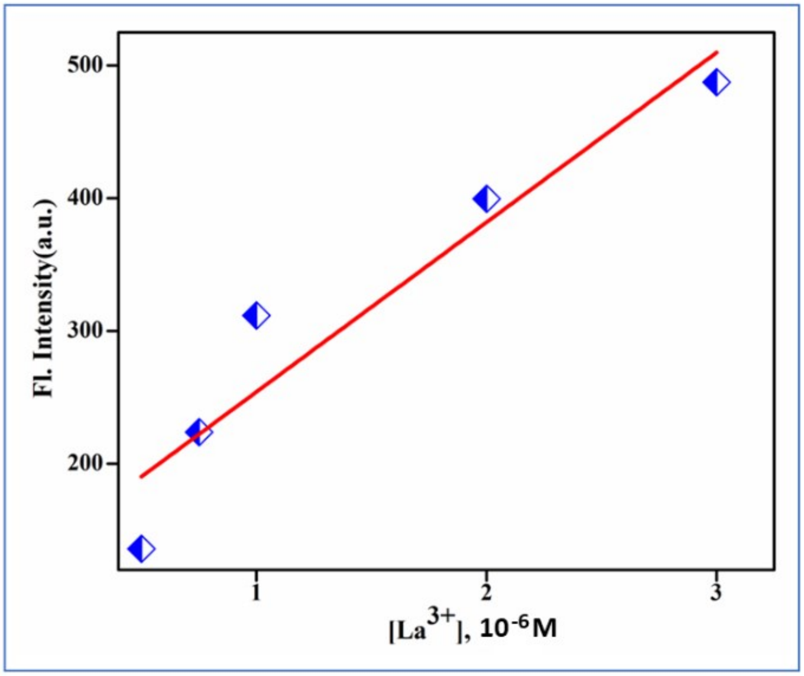

Fig. S13 Liner region of **Fig. S12**

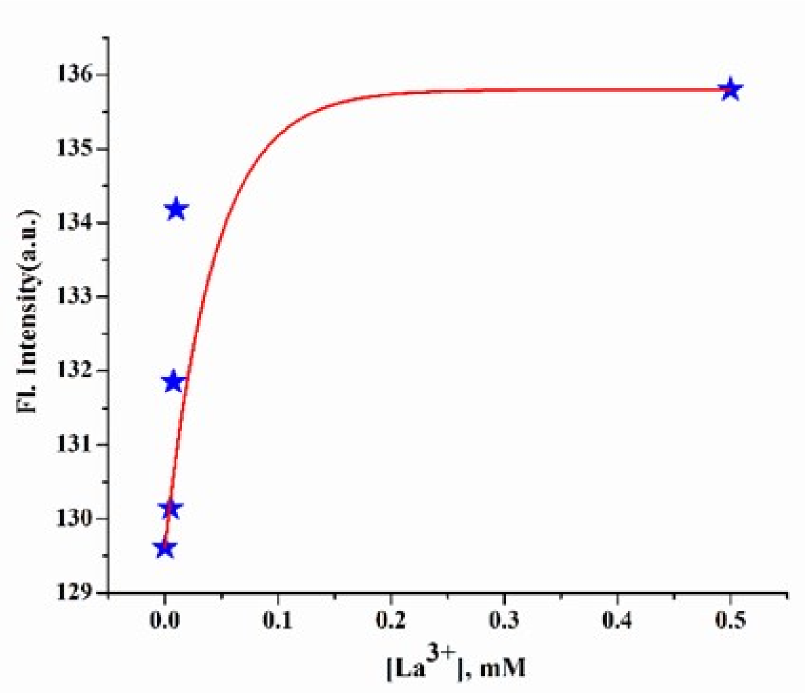

Fig. S14 Plot revealing practical detection limit

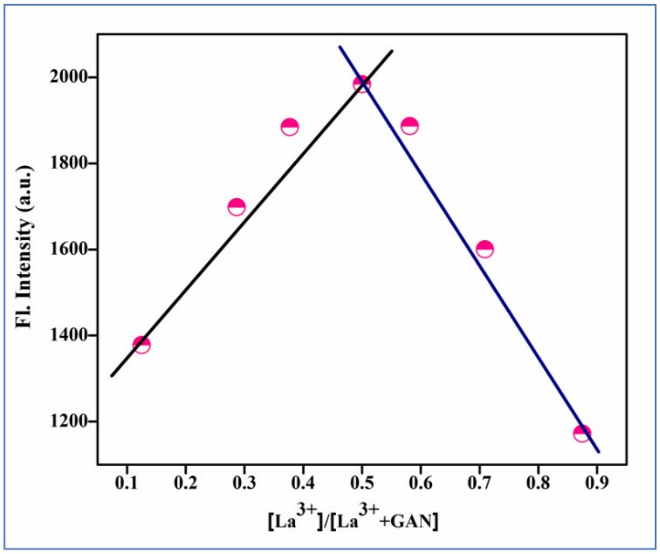

Fig. S15 Job's plot for determination of stoichiometry of interaction between **GAN** with La^{3+} (λ_{ex}, 336 nm)

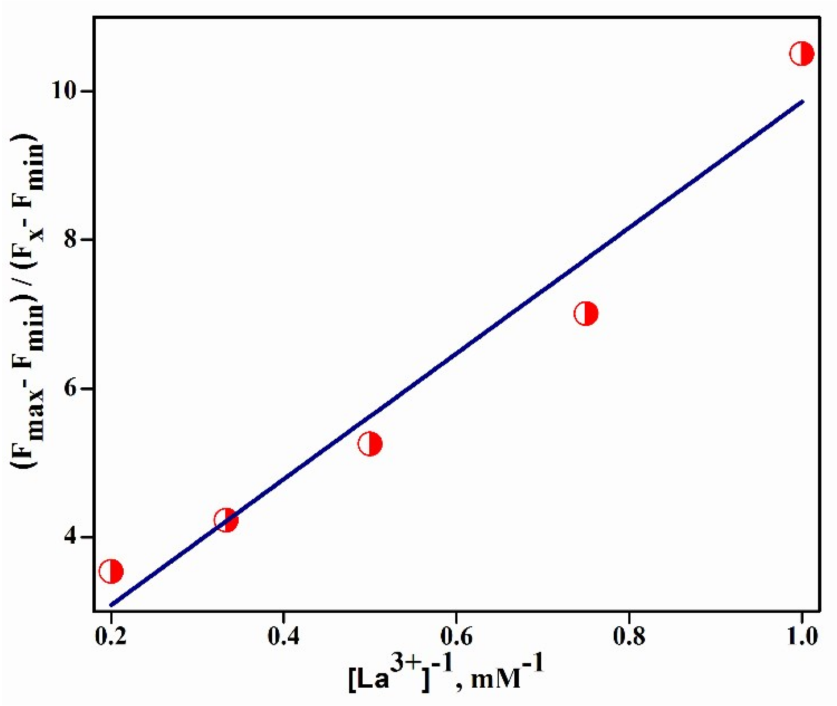

Fig. S16 Benesi−Hildebrand plot for determination of association constant between **GAN** and La^{3+} ion

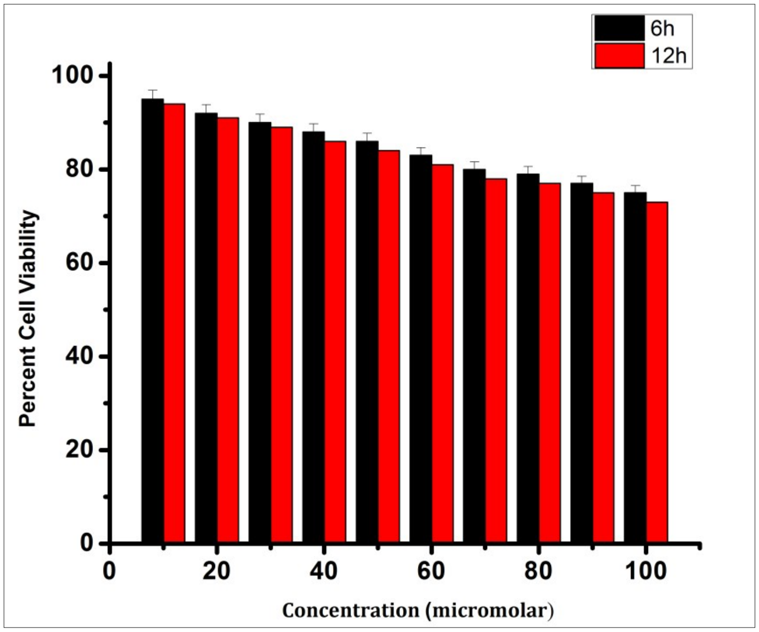

Fig. S17 Cell viability of **GAN** at different concentration against HeLa cells after 12h incubation.

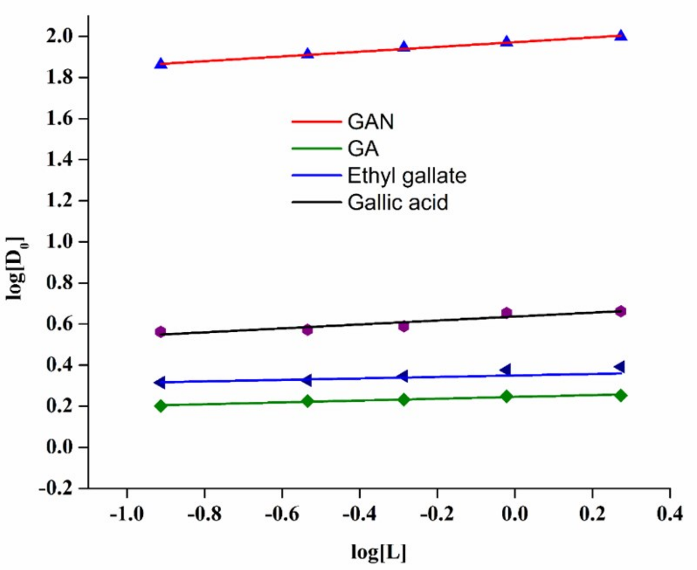

Fig. S18 Comparative extraction ability of gallic acid (G), GA, **GAN**, and ethyl gallate for La^{3+}

Table S1 Crystallographic parameters of the **GAN**

	GAN
CCDC	1889365
System	Orthorhombic
Space Group	P 21/n
a/Å	9.1843
b/Å	14.6445
c/Å	12.5246
α/°	90
β/°	102.665
γ/°	90
Volume/Å3	1643.56
Z	4
T/K	150
Dx/ gm cm^{-3}	1.513
Mu (mm-1)	0.118
F000	784.0
F000′	748.46
h, k, l max	11, 17, 15
N$_{ref}$	3135
T$_{min}$, T$_{max}$	0.972, 0.995
Data completeness	1.000
Theta max	25.723
R(reflections)	0.0444(2112)
wR2(reflection)	0.1126(3135)
S	1.026
N$_{par}$	280

Table S2 Selected bond angles and lengths of **GAN**

Atoms	Angles	Atoms	Distance
C1 O1 H1A	105.5	O1 C1	1.361
C15 O3 H3A	110	O1 H1A	1.11
C16 O4 H4A	111	O2 C12	1.239
C17 O5 H5A	111.8	O3 C15	1.368
C11 N1 N2	116.87	O3 H3A	0.93
C12 N2 N1	119.52	O4 C16	1.367
C12 N2 H2A	124.0	O4 H4A	0.93
N1 N2 H2A	116.2	O5 C17	1.365
O1 C1 C10	121.8	O5 H5A	0.92
O1 C1 C2	116.7	N1 C11	1.295
C10 C1 C2	121.5	N1 N2	1.376
C3 C2 C1	120.0	N2 C12	1.348
C2 C3 C4	121.6	N2 H2A	0.84
C5 C4 C3	121.7	C1 C10	1.390
C5 C4 C9	119.3	C1 C2	1.405
C3 C4 C9	119.1	C2 C3	1.358
C6 C5 C4	121.5	C3 C4	1.414
C5 C6 C7	119.3	C4 C5	1.413
C8 C7 C6	121.1	C4 C9	1.419
C7 C8 C9	121.0	C5 C6	1.363
C8 C9 C4	117.8	C6 C7	1.397
C8 C9 C10	123.0	C7 C8	1.370
C4 C9 C10	119.1	C8 C9	1.416
C1 C10 C11	121.2	C9 C10	1.443
C1 C10 C9	118.7	C10 C11	1.440
C11 C10 C9	120.08	C12 C13	1.486
N1 C11 C10	120.8	C13 C18	1.395
O2 C12 N2	121.2	C13 C14	1.396
O2 C12 C13	121.85	C14 C15	1.386
N2 C12 C13	116.96	C15 C16	1.390
C18 C13 C14	119.7	C16 C17	1.393
C18 C13 C12	116.98	C17 C18	1.384
C14 C13 C12	123.25	O100 H10A	0.88
C15 C14 C13	119.5	O100 H10B	0.83
O3 C15 C14	123.6	O200 H20A	0.91
O3 C15 C16	115.7	O200 H20B	0.840
C14 C15 C16	120.7		
O4 C16 C15	121.48		
O4 C16 C17	118.8		
C15 C16 C17	119.7		
O5 C17 C18	123.6		
O5 C17 C16	116.46		

C18 C17 C16	119.9		
C17 C18 C13	120.4		
H10A O100 H10B	111		
H20A O200 H20B	96		

Table S3 Comparison among pioneering La^{3+} sensors

Probes	**Media**	**Binding constant (M^{-1})**	**LOD (M)**	**Ref.**
2,3,6,7,10,11-hexa(2-pyridyl)-dipyrazino [2,3-f:2',3'-h]quinoxaline (HPDQ),	CH_3CN	------	$5x10^{-5}$	1
Albendazole (ABZ)	CH_3OH	--------	$1.9X10^{-8}$	2
5FU (5-fluorouracil)	HPLC mobile phase (70% methanol and 30% Milli-Q)	$0.364x10^{4}$	$19.29X10^{-6}$	3
GAN	**DMSO/ H_2O (4 /1)**	**$1.1×10^{5}$**	**$23.93×10^{-9}$**	**Present work**
Bis(thiophenal)phenylen-1,3-diamine (TPD)	H_2O	-----------	$2.0 × 10^{-8}$	4

References

1.Q. Zhao, X. M. Liu, H. R. Li, Y. H. Zhang and X. H. Bu, *Dalton Trans.*, 2016, **45**, 10836

2. A. A. Hamad, R. Ali, H. R. H. Ali, D. M. Nagyc and S. M. Derayea, *RSC Adv.,* 2018, **8**, 5373

3. N. A. El-Maali, A. Y. Wahman, A. A.M. Aly, A. Y. Nassar and D. M. Sayed, *Appl Organometal Chem.,* 2020; e5594

4. M. R. Ganjalia, M. Qomib, A. Daftaria, P. Norouzia, M. Salavati-Niasaric and M. Rabbania, *Sensors and Actuators B*, 2004, **98**, 92–96.

Table S4 Effect of catalyst load and solvent on the yield of benzimidazole derivative

Entry	**Catalyst load (mg)**	**solvent**	**Yield (%)**
1	10	Ethanol	95
2	10	Methanol	82
3	10	Acetonitrile	69
4	05	Ethanol	68
5	15	Ethanol	95
6	00	Ethanol	22[a]

Reaction conditions: *o*-phenylenediamine (1 mmol), benzaldehyde (1 mmol), solvent (5 mL), room temperature, time, [a]reaction time, 24h.

Table S5 Effect of substituent on aldehyde to product yield (%)

Entry	**Aldehyde**	**Product**	**Yield (%)[a]**
1	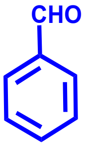	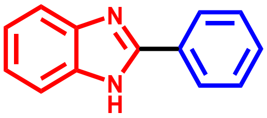	**95**
2	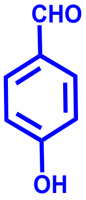	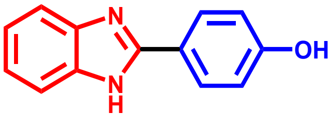	**90**
3	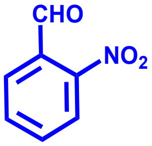	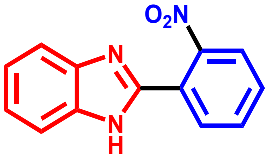	**88**
4	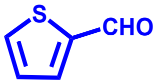	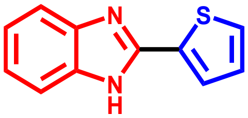	**84**
5	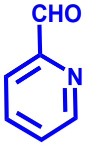	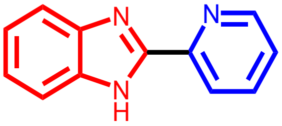	**83**

Reaction: *o*-Phenylenediamine (1 mmol); benzaldehyde (1 mmol); ethanol (5 mL); room temperature; time, 45 minute; [a] isolated yield**.**

Table S6 La^{3+} extraction efficiency (%) of G, GA, **GAN** and ethyl gallate

Compounds	**% of extraction**
GAN	98.92
G	64.00
GA	81.87
Ethyl gallate	75.18

Table S7 Comparison among pioneering La^{3+} extractants

Ligands	**Solvent**	**% Extraction**	**Ref.**
Tricaprylmethylammonium chloride (A336) and *sec*-Octylphenoxy acetic acid (CA-12)	Toluene	75.2 ± 2.1	1
Tricaprylmethylammonium chloride (A336) and *sec*-nonylphenoxy acetic acid (CA-100)	Toluene	79.1 ± 2.3[1]	1
18-Crown-6	2-Thenoyltrifluoroacetone	--	2
Bis(benzo-15-crown-5)	Dichloromethane (DCM)	18.2	3
Di-(2-ethylhexyl) Phosphoric Acid	Kerosene	---	4
Methanesulphonic acid	Di-(2-ethylhexyl)phosphoric acid	77.1	5
GAN	Ethylacetate	98.95	**Present work**

References

1 W. Wang, H. Yang, H. Cui, D. Zhang, Y. Liu and J. Chen, *Ind. Eng. Chem. Res.,* 2011, **50**, 7534-7541.

2 N. Hirayama, H. Okamura, K. Kidani and H. Imura, *Anal. Sci.*, 2008, **24**, 697-699.

3 Y. Inoue, S. K. Nakagawab and T. Hakushi, *J. Chem. Soc., Dalton Trans.,* 1993, 2279-2281.

4. S. Yin, W. Wu, X. Bian, Y. Luo and F. Zhang, *Int. J Nonferrous Metal.*, 2013, **2**, 75-79.

5. L. Gijsemans, F. Forte, B. Onghena and K. Binnemans, *RSC Adv.***,** 2018, **8**, 26349-26355.